MDB-7 | 67

MILITARY TECHNICAL COLLEGE
CAIRO - EGYPT

CYCLIC PLASTIC DEFORMATIONS IN THIN TUBES UNDER BILINEAR RADIAL THERMAL GRADIENT

M.M. MEGAHED*

ABSTRACT

The cyclic plastic behaviour of thin walled tubes subjected to internal pressure and cyclic radial thermal gradient is investigated. Such structural problems find many applications in high temperature nuclear plants, conventional power plants and chemical industries where the integrity of mechanical components is governed by growth of inelastic strains due to plastic ratchetting and time dependent creep as well as the interaction between creep damage and low cycle fatigue damage.

The tube problem is treated analytically with the aid of an approximate uniaxial model which compensates the effects of axial stress by magnifying the thermal stress in the hoop direction. The model is shown to provide conservative estimates of observed strains. Linear kinematic hardening material model is used in the plastic analysis and an approximate technique is employed to account for the cyclic hardening phenomena. Emphasis is placed upon the effects of the non-linear temperature distribution since ratchetting tests on thin tubes have shown that the observed temperature distribution is far from linear. The results of the analysis show that the bilinear form of radial temperatures introduces new modes of cyclic deformation in which cyclic plasticity is confined to the inner skin of the tube wall.

The results are compared with test data on AISI 304 stainless steel tubes under internal pressure and cyclic thermal shocks between 1100 °F and 800 °F with hold periods of 160 hr/cycle at 1100 °F. The stress fields obtained from rapid cycle solutions are used to estimate upper bounds for creep deformations which accumulate during the hold periods. The predictions of plastic and creep strains are seen to provide moderate conservative estimates of test results.

*Assistant Prof.,College of Eng.King Abdulaziz University P.O.Box 9027, Jeddah, Saudi Arabia

*On leave from: Dept.Mech.Design and Production,Cairo University, Giza, Egypt.

INTRODUCTION

Many pressure vessels and pipes are subjected to mechanical loads due to pressure or dead weights upon which cyclic thermal loads are superimposed. The cyclic thermal loads are caused by fluctuations in the temperature of the fluid within the vessel. Research into the inelastic behaviour of structural components under cyclic thermal stresses has witnessed a growing interest in recent years due to its vital importance to the design of the components of high temperature nuclear plants. The ultimate goal of this research is to provide the designer with rules which enables him to assure a level of structural integrity consistent with the high levels of safety required for nuclear equipment.

Recent work [1] into the effects of combined mechanical and thermal stresses on the behaviour of structural components has shown that such situations lead to a variaty of responses. The simplest response is the elastic one which occurs for low magnitudes of stresses. If the stresses exceed yield,several possibilities arise. First, the structure may shakedown to an elastic state of deformation after an initial excursion into the plastic regime during the first few cycles; the behaviour during subsequent cycles is purely elastic. Second , the structure may incur cyclic alternating plasticity in which plastic strains are applied and removed and failure eventually occurs due to low cycle fatigue. Finally, the third possibility is that ratchetting could occur. This results in accumulation of plastic strain increments during each load cycle. This may eventually lead to unacceptable changes in the dimensions of the component. Hence, operating stresses should be chosen such that ratchetting is minimized.

The origin of the ratchetting phenomenon described above lies in the cyclic interaction between elastic and plastic strains. Hold periods at elevated temperatures cause additional accumulation of inelastic strains due to time dependent creep strains. Creep may also enhance plastic ratchetting due to the accompanying stress relaxation. Further, creep damage is superposed upon existing fatigue damage and consequently the failure of the component is enhanced.

Early theoretical work into the ratchetting problem utilized simple structural models such as two bar analogues and perfectly plastic materials as adopted by Parkes [2] in his investigation of aircraft Wings. Miller [3] , Burgreen [4] and Bree [5] considered a thin tube under cyclic linear thermal gradient across its wall. Approximate uniaxial model and perfect plasticity assumptions are used in order to facilitate analytical treatment. However, tubes used in high temperature reactor applications are made from Austenitic stainless steels which exhibit considerable strain hardening as well as cyclic hardening, cyclic creep and cyclic relaxation under conditions of reversed strain [6]. Mulcahy [7] and Megahed [8] investigated the influence of hardening models on

the ratchetting behaviour using two of the most commonly used plasticity theories; viz; isotropic hardening and kinematic hardening. Isotropic hardening represents a full cyclic hardening material while kinematic hardening represents a material which does not harden due to load cycles but exhibits the observed Bauschinger effect.

Experimental work into the ratchetting problem has been in progress over the last decade in U.S.A, U.K, Japan and France. Uga [9] tested stainless steel specimens which simulate two-bar structures under cyclic thermal stresses. Corum et al [10] tested thin walled tubes under internal pressure and cyclic thermal shocks across its wall. Yamamoto et al [11] tested thin steel tubes under axial stress and cyclic thermal gradient across the wall. Megahed et al [12] , [13] conducted a number of tests on simulated two bar structures made from commercially pure copper and AISI 316 stainless steel. These tests have shown that cyclic creep induces an additional component of ratchetting which does not decay with load cycles as predicted by classical theories of plasticity. Cyclic hardening has been shown to have some undesirable effects on the ratchetting limits predicted by classical theories.

Previous work has illucidated the effects of work-hardening [7,8] and the cyclic phenomena of metals [12,13] on the ratchetting behaviour. Hence, reliable predictions of the ratchetting response must take these aspects of the material behaviour into account. In the present work, a thin tube under cyclic non-linear radial temperature distribution is considered. The non-linear distribution of temperature is approximated by means of bilinear relation which represents in a faithful manner the observed temperature distributions in ratchetting tests on thin tubes [10]. The problem is investigated analytically by reducing the two-dimensional elasto-plastic problem into a uniaxial one which is shown to yield conservative estimates of ratchet strain. Linear kinematic hardening plasticity theory and an associated approximate method which accounts for cyclic hardening are used in the analysis. The cyclic plastic strains are governed by a set of recurrence relations which are evaluated numerically. The cyclic plastic solutions for the stress fields are used to estimate upper bounds on creep deformations which accumulate during hold periods at elevated temperatures [14,15].

The results of the present work are compared with test data [10] on thermal ratchetting of 304 stainless steel tubes subjected to thermal shocks between 1100 °F and 800 °F with 160 hr hold period per cycle at 1100 °F. The predictions are shown to provide moderate conservative estimates of observed ratchet strain. The origin of the conservatism is traced back to the reduction of the biaxial problem into an approximate uniaxial one.

THE THERMO-ELASTIC PROBLEM

A thin-walled tube of inner radius a, outer radius b is subjected to an internal pressure p and a cycle of radial thermal gradient of maximum amplitude T_o distributed bi-linearly across the wall thickness t such that the temperature is cycled between zero and T(x) where,

$$T(x) = - T_o \langle x-h \rangle / (1-h) \qquad (1)$$

where x=(b-r)/t; i.e. x=0 at the outer radius and x=1 at the inner radius. The function $\langle x-h \rangle = 0$ for $0 \leq x \leq h$ and $\langle x-h \rangle = x-h$ for $h \leq x \leq 1$. The amplitudes of the corresponding elastic thermal stresses are given by [16]:

$$\sigma_\theta = \sigma_z = - \frac{E\alpha T_o}{2(1-\nu)} [(1-h)-2 \langle x-h \rangle / (1-h)] \qquad (2)$$

These stresses are superimposed upon the membrane stresses due to internal pressure;

$$\sigma_\theta = 2\sigma_z = PD/(2t) \qquad (3)$$

where D is the mean diameter of the tube.

As argued by Bree [5] , the two-dimensional tube problem can be reduced to an equivalent uniaxial problem which predicts conservative estimate of plastic strains. This is achieved by ignoring the effect of σ_z since its effect on accumulation of plastic strain is opposite to that of the larger σ_θ . On the basis of this approximation, it can be shown that the equivalent uniaxial model is that of a slab prevented from bending and subjected to a steady mechanical stress $\sigma_p = PD/(2t)$ in addition to a temperature cycle which varies between zero and,

$$T(x) = - \frac{T_o}{1-\nu} \langle x-h \rangle / (1-h) \qquad (4)$$

as illustrated in Fig.1. The corresponding elastic thermal stresses are:

$$\sigma(x) = - \frac{E\alpha T_o}{2(1-\nu)} [(1-h)-2 \langle x-h \rangle / (1-h)] \qquad (5)$$

which is the same as eq. (2). An operating condition of the tube can be defined in terms of σ_p , σ_t where

$$\sigma_p = \frac{PD}{2t} , \quad \sigma_t = \frac{E\alpha T_o}{2(1-\nu)} \qquad (6)$$

as shown in Fig.1. Elasto-plastic analyses of this problem are now discussed.

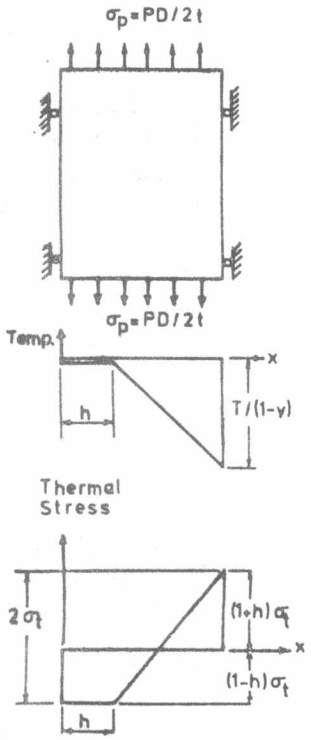

Fig.1 Equivalent uniaxial model

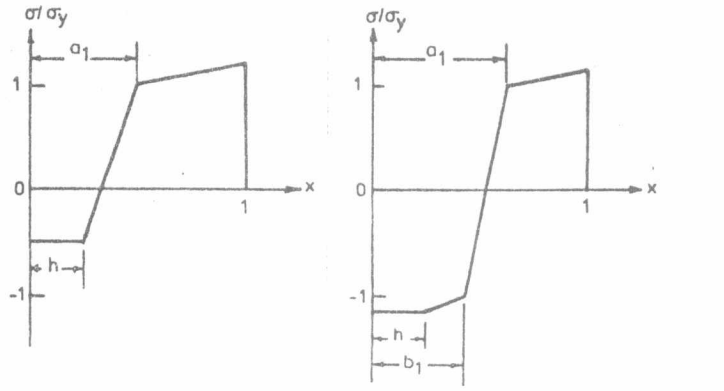

a) Tensile yielding only b) Tensile and compressive yielding

Fig.2 Stresses during the first half cycle

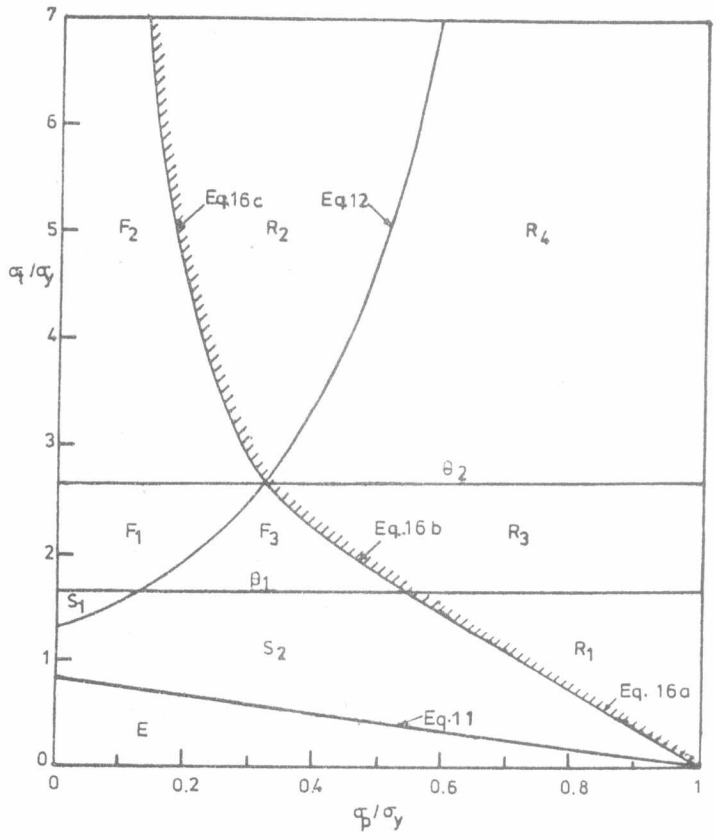

Fig. 3 Modes of behaviour for a uniaxial tube model (K=40, h=0.2)

E	Fully elastic behaviour
S_1, S_2	Elastic shakedown
F_1, F_2, F_3	Cyclic plasticity
R_1, R_2, R_3, R_4	Ratchetting

ELASTO-PLASTIC ANALYSIS

The elasto-plastic analysis is carried out using a linear kinematic hardening plasticity theory. The slope of the plastic protion of the stress-strain curve is assumed to have a constant value of βE (β= 0.01-0.05 for most strain hardening materials). Therefore, the flow rule is,

$$\frac{d\varepsilon_p}{d\sigma} = \frac{1-\beta}{\beta E} = \frac{K}{E} \quad , \quad K = \frac{1-\beta}{\beta} \tag{7}$$

For simplicity all material properties, E, α, ν, K and σ_y are assumed to be independent of temperature.

Initially, the model is subjected to the uniform stress σ_p at the isothermal condition T(x) = 0. Upon application of first cooling, eq. (4) the stresses will increase at the cold fibers and decrease at the hotter ones. Hence, two distinct elasto-plastic stress fields will arise; the first field involves tensile yielding at the cold fibers $a_1 \leq x \leq 1$, (Fig. 2a) and the second field involves both tensile yielding at $a_1 \leq x \leq 1$ and compressive yielding at $0 \leq x \leq b_1$, (Fig.2b) where a_1 , b_1 are the elasto plastic fronts.

The stress-strain relations applicable to the tensile yielding stress field are:

$$\varepsilon_1 = [\sigma(x) - 2\sigma_t \langle x-h \rangle/(1-h)]/E \quad \text{for} \quad 0 \leq x \leq a_1$$

$$\varepsilon_1 = [\sigma(x) - 2\sigma_t \, (x-h)/(1-h) + K(\sigma(x)-\sigma_y)]/E \quad \text{for} \quad a_1 \leq x \leq 1 \tag{8}$$

where the total strain ε_1 is assumed to be the sum of the elastic, thermal and plastic components. Satisfaction of the equilibrium and compatibility conditions:

$$\sigma_p = \int_0^1 (x).dx \ , \ \varepsilon_1 = \text{constant} \tag{9}$$

provides the means for determining ε_1 and a_1 as:

$$\varepsilon_1 = [\sigma_y - 2\sigma_t (a_1-h)/(1-h)]/E \tag{10a}$$

$$a_1 = \frac{1}{K}\left[-1 + \sqrt{(1+K)(1+Kh^2) + K(1+K)(1-h)(1-\sigma_p/\sigma_y).\sigma_y/\sigma_t}\right] \tag{10b}$$

The expression for a_1 can be used to identify the operating conditions corresponding to the two stress fields shown in Fig.(2). For example, simultaneous tensile compressive yielding occurs if $\sigma(0) \leq \sigma_y$ and fully elastic behaviour occurs if $a_1 \leq 1$. After substitutions, these conditions are expressed in terms of σ_p , σ_t as:

$$\sigma_p/\sigma_y \leq [-(1+h)\ \sigma_t/\sigma_y \qquad (11)$$

for the full elastic behaviour (E) and

$$\frac{\sigma_p}{\sigma_y} \leq \frac{1-h}{1+k}\left[\frac{\sigma_t}{\sigma_y} - K\,\frac{\sigma_y}{\sigma_t}\right] + \frac{K-2Kh-1}{1+K} \qquad (12)$$

for the stress field shown in Fig. (2b). In a similar manner, the solution for the stress field shown in Fig.(2b) is obtained as:

$$\varepsilon_1 = [\sigma_y - 2\sigma_t(a_1-h)/(1-h)]/E = [-\sigma_y - 2\sigma_t(b_1-h)/(1-h)]/E \qquad (13a)$$

$$a_1 = \frac{(1+h^2)\sigma_t/\sigma_y - (1-h)(1+K)(1-\sigma_p/\sigma_y) + K(1-h)^2.\sigma_y/\sigma_t}{2[\sigma_t/\sigma_y + K(1-h)]} \qquad (13b)$$

Analysis of subsequent cycles shows that the model may exhibit shakedown or ratchetting. Shakedown may be elastic in regions S_1 , S_2 or plastic in regions F_1 , F_2 , F_3 as shown in Fig.(3) which is known as the Bree diagram. Ratchetting or incremental strain growth takes place in the regions denoted R_1 , R_2, R_3 and R_4.

SHAKEDOWN

Plastic shakedown involves cyclic plasticity which leads to the failure of the component due to low cycle fatigue. The three stress fields shown in Fig. (4) show the modes of cyclic plasticity present in the uniaxial model. Cyclic plastic deformation takes place at $b_2 \leq x \leq 1$ (i.e. at the inner skin of the tube) for the modes F_1 , F_3 illustrated in Figs. (4a,b) respectively. In Fig. (4c), cyclic plasticity takes place at both the inner ($b_2 \leq x \leq 1$) and outer ($0 \leq x \leq a_2$) skins of the tube. Regions F_1 , F_2 and F_3 are shown in the Bree diagram of Fig. (3). The boundary between (F_1 , F_3) and F_2 can be determined from the condition that a_2 (in Fig. 4c)$\leq h$ which guarantees the confinement of cyclic plasticity to the inner skin of the tube. This boundary is obtained as:

$$\sigma_t/\sigma_y = \frac{1}{1-h}\left[\sqrt{(K-2Kh-1)^2 + 4K(1-h)^2} - (K-2Kh-1)\right] = \theta_2 \qquad (14)$$

Elastic shakedown (regions S_1 , S_2) takes place if the plastic front b_2 (in Figs. 4a,b) exceeds x=1. This results in purely elastic behaviour during subsequent cycles. The boundary between (F_1,F_3) and (S_1,S_2) is obtained as:

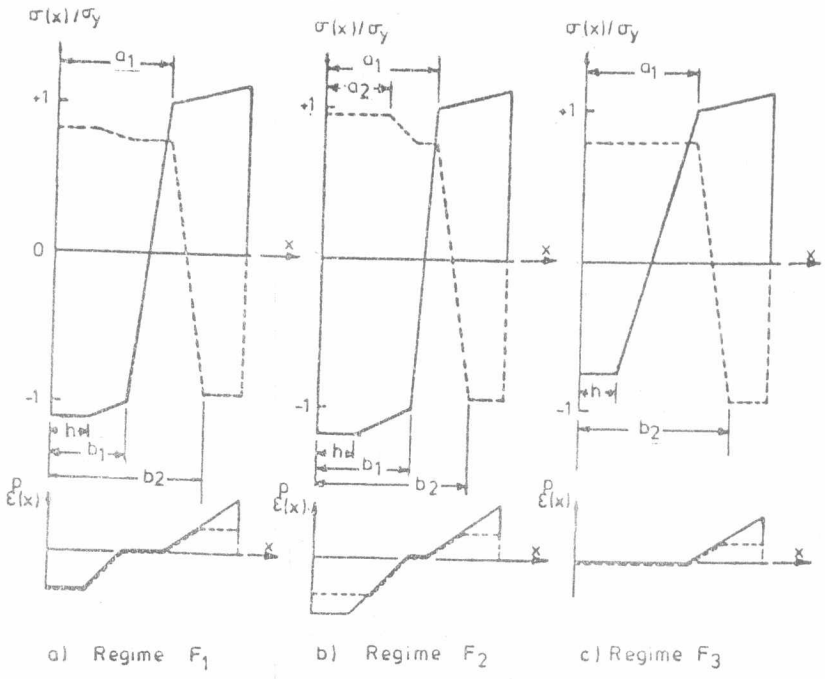

Fig.4 Cyclic plasticity regimes, cyclic-stress fields and plastic strains(——cooling, --- heating).

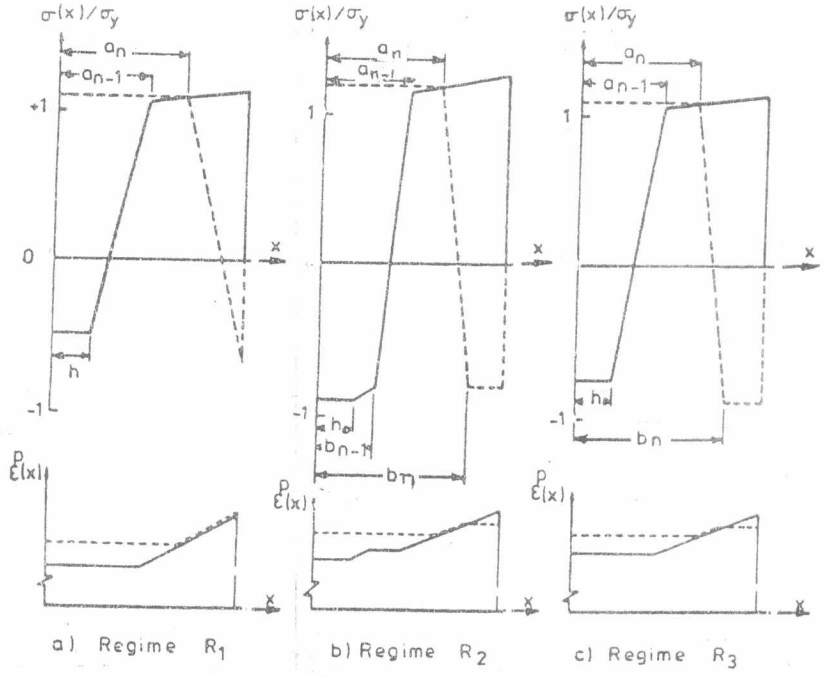

Fig.5. Ratchetting regimes, transient cyclic stress and plastic strain fields(—— Cooling,---heating).

6

$$\sigma_t/\sigma_y = \frac{2}{1-h} = \theta_1 \tag{15}$$

Elastic shakedown is a viable mode for operation while in plastic shakedown, accumulation of fatigue damage should be checked. Note that for linear temperature distribution(h=0), $\theta_1 = \theta_2 = 2$ which is the classical result of Bree [2].

RATCHETTING

Considerations of the stress fields present in regions S_2,F_3 and F_2 show that cyclic growth of plastic strains will take place[2] if the core stress during first heating (Fig.4) exceeds the initial yield stress σ_y. After some manipulations, the ratchetting limit is determined as:

$$\sigma_p^*/\sigma_y = 1 - \frac{K(1+h)(1-h^2)}{4(1+K)}\,\sigma_t/\sigma_y, \quad \text{for } 0 \leq \frac{\sigma_t}{\sigma_y} \leq \theta_1 \tag{16a}$$

$$\sigma_p^*/\sigma_y = \sqrt{\frac{(1+Kh^2)\sigma_t/\sigma_y + 2K(1-h)}{(1+K)\sigma_t/\sigma_y}} - \frac{(1+K)\sigma_t/\sigma_y + K(1-h)}{(1-K)\sigma_t/\sigma_y}$$

$$\text{for } \theta_1 \leq \frac{\sigma_t}{\sigma_y} \leq \theta_2 \tag{16b}$$

$$\sigma_p^*/\sigma_y = \frac{(1+Kh^2)\sigma_t/\sigma_y + 3K(1-h) + 2K^2(1-h)^2.\sigma_y/\sigma_t}{(1+K)\ \sigma_t/\sigma_y + 2K\ (1-h)} \quad \text{for } \frac{\sigma_t}{\sigma_y} \geq \theta_2 \tag{16c}$$

as illustrated in Fig. (3).

Four distinct ratchetting mechanisms are present, viz. R_1,R_2 R_3 and R_4. The transient stress fields during a typical cycle N(as defined by the nth heating and (n-1) th cooling where n=2N) are illustrated in Fig.(5) for the mechanisms R_1,R_2 and the second stage of R_3. The plastic fronts a_i and the corresponding increments of strain are obtained by evaluating the recurrence relations given in the flow diagram of Fig.(6). In regime R_1 , elastic shakedown is approached at the steady state when $a_n = a_{n-1} \to a_\infty$ and $\Delta\varepsilon \to 0$. In regime R_2, accumulation of ratchet strain is accompanied by cyclic plasticity at both the inner ($b_n \leq x \leq 1$) and outer ($0 \leq x \leq b_{n-1}$) skins of the tube. In regime R_3 , ratchetting takes place according to two consecutive phases; the mechanism R_1 is adopted at first until sufficient degree of hardening is developed which allows compressive yielding to take place during heating half cycles

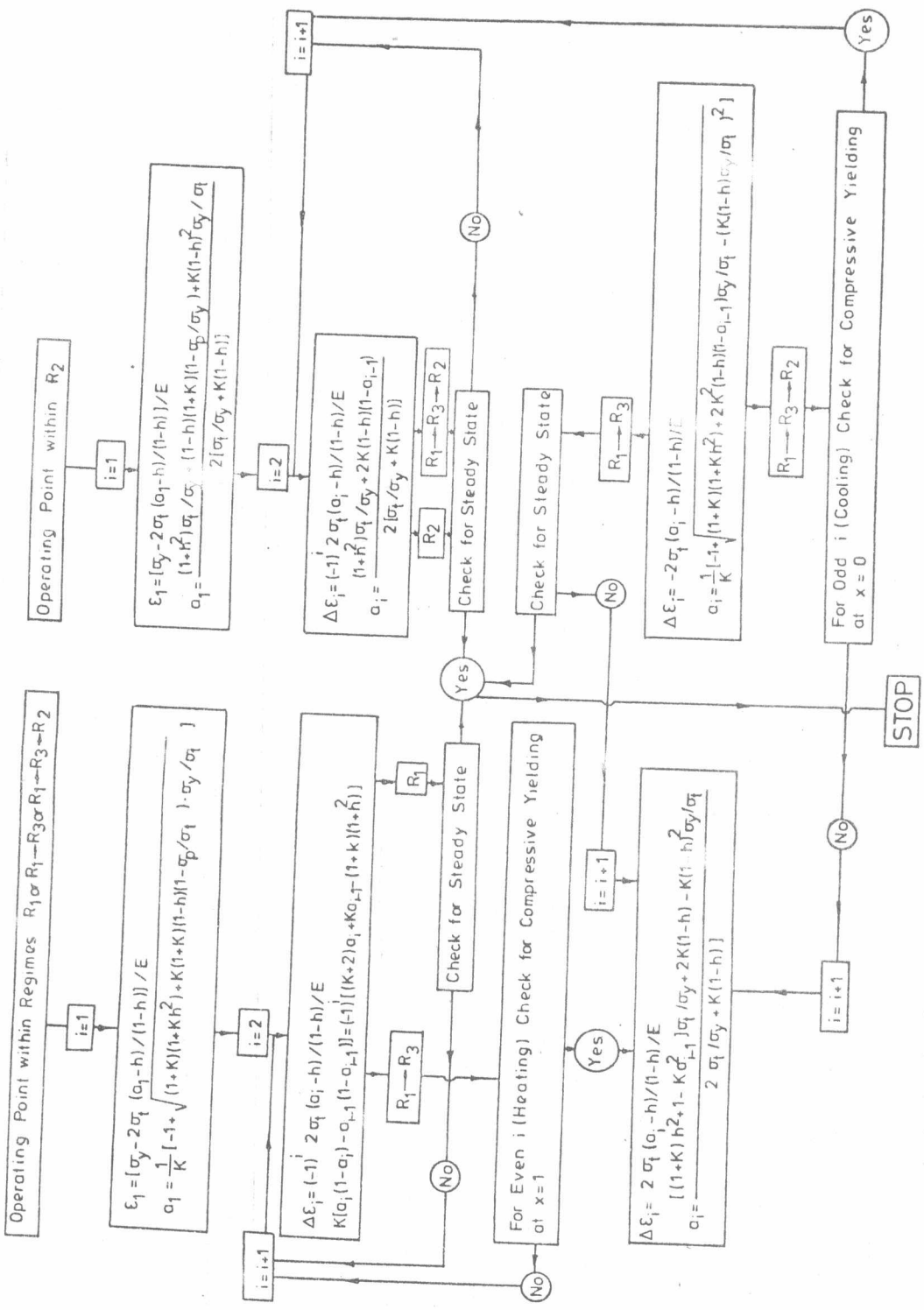

Fig.6. Flow diagram for calculation of ratchet strain.

as shown in Fig. (5c). Subsequent ratchetting is accompanied by cyclic plasticity at the inner skin ($b_n \leq x \leq 1$) of the tube. Similarly, regime R_4 consists from three consecutive ratchetting mechanisms identified as R_1, R_3 and R_2. It is evident that the steady state of regimes R_2 , R_4 will be a plastic shakedown state similar to F_2 (Fig. 4c) and the steady state of regime R_3 will be similar to that present in the plastic shakedown mode F_3 (Fig. 4b).

Numerical examples obtained using the algorithm given in Fig. (6) for the accumulation of ratchet strains according to R_1, R_2, R_3 and R_4 are shown in Fig. (7). It is evident that a cyclic steady state is reached after 30 cycles for K = 40 which characterizes the hardening behaviour of austenitic steels. An overall picture of the results may be gained from the contours of asymptotic ratchet strains as shown in Fig. (8) for a thin walled tube made from 304SS and subjected to thermal shocks. It is noted that the contours are almost parallel to the ratchet limit σ_p^*/σ_y and hence ratchet strains are more sensitive to changes in pressures than temperatures.

An important set of result which emerge from the present work is the effect of the bilinear distribution of thermal gradient on the plastic behaviour of the model. For lienar distribution (h=0) , the plastic shakedown modes F_1 , F_3 and the ratchetting regime R_3 are not present as may be seen from calculation of θ_1 , θ_2 for h = 0 (eqs. (14)). Hence, new modes of deformation are introduced for h >0 in which cyclic plasticity is confined to the inner skin of the tube only as compared to cyclic plasticity at both the inner and outer surfaces of the tube for h=0. Figure (9) shows the effect of the value of h on ratchet strain and amplitudes of cyclic plasticity at typical operating conditions. It is observed that ratchet strain increases with h until a maximum value is reached. The effect of h on cyclic plasticity is quite prominant, e.g. $\Delta\varepsilon_p(0) = \Delta\varepsilon_p(1) = 1.5\ \sigma_y/E$ at h=0 while $\Delta\varepsilon_p(0) = 0$ $\Delta\varepsilon_p(1) = 3 \cdot \sigma_y/E$ at h=0.3 for $\sigma_t/\sigma_y = 3.5$. Hence, the bilinearity of thermal gradient doubles $\Delta\varepsilon_p(1)$ which in turn reduces the fatigue life considerably. Further, examination of the ratchet limit as defined by σ_p^*/σ_y shows that the likelyhood of ratchetting is enhanced for h>0.

Perfect plasticity solution can be generated from kinematic hardening results by letting $K \to \infty$. In such case, ratchet strains accumulate in equal increments per cycle. There will be three distinct ratchet mechanisms; R_1, R_2 and R_3. Obviously, the change from one mechanism of ratchetting to another will not be present since it is a direct consequence of strain hardening.

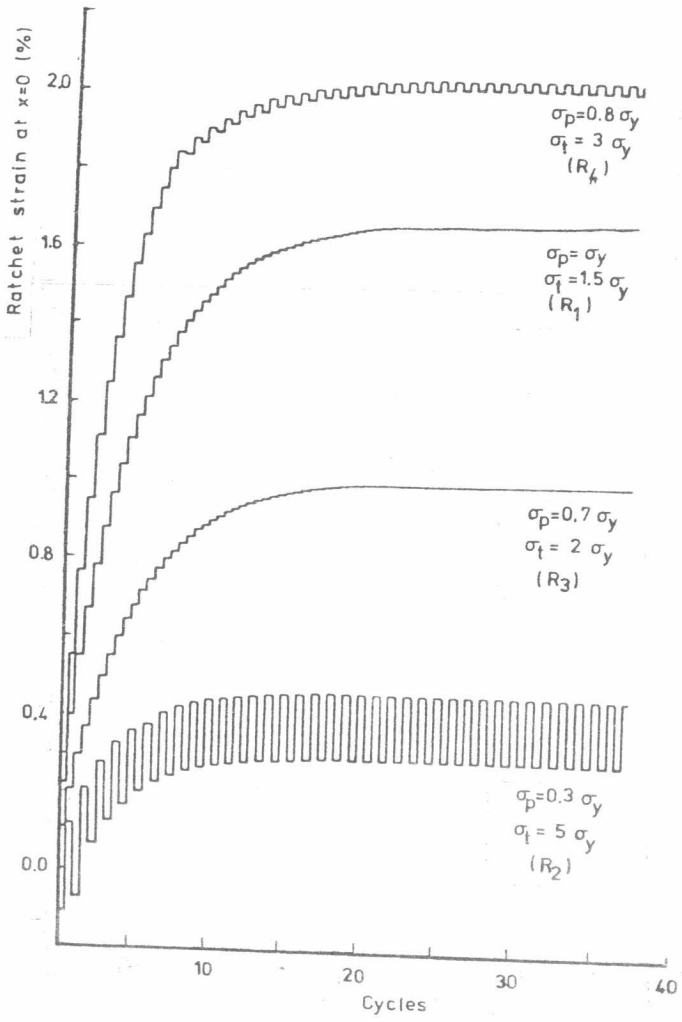

Fig. 7

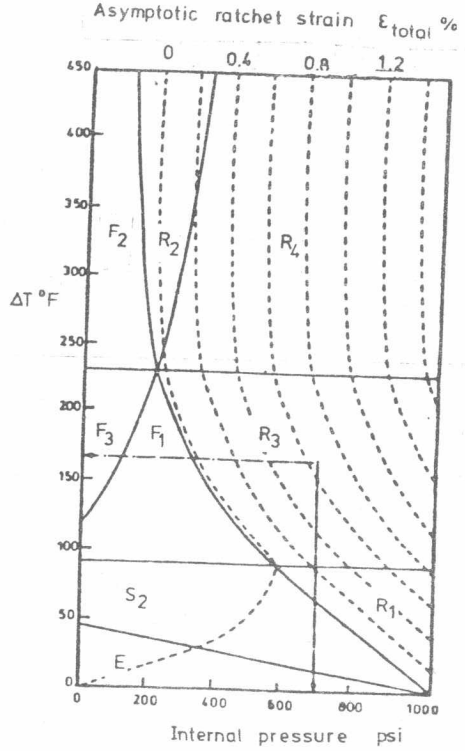

Fig. 8

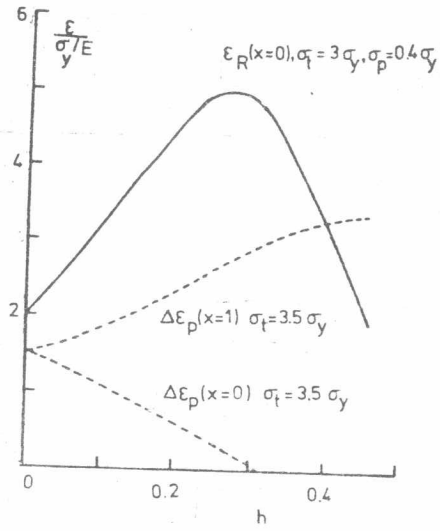

Fig. 9

Fig.7. Examples of ratchet strain accumulation (K = 40, h = 0.2, σ_y/E = 0.1%).

Fig.8. Full solution map and contours of total ratchet strain for a tube (D/t= 21.5, h = 0.328) using monotonic properties of 30455 at 900 °F [σ_y=11.15 KSi, E=23.3x10^6 psi, α = 11x10^{-6}/°F, K = 38.56, ν=0.3)]

Fig.9. Effect of h on ratchet strain and amplitudes of cyclic plasticity.

FIRST A.M.E. CONFERENCE
29-31 May 1984, Cairo

6

COMPARISON WITH TEST RESULTS

Corum et al [10] conducted thermal ratchetting tests on a 304 stainless steel tube with D/t = 21.51. The tube is subjected to 13 thermal downshocks between 1100 °F and 800 °F in a sodium loop under internal pressure of 700 psi as shown in the load histogram of Fig. (10a). There is a hold period of 160 hrs at 1100 °F between each two consecutive shocks. The temperature distribution across the tube wall is recorded with time as shown in Fig. (10b). The thermal gradient attains a maximum value of 167 °F after 12 seconds from the start of the shock. The nonlinear temperature distribution may be approximated by a bilinear distribution according to eq. (1) with h = 0.328.

The results presented in earlier sections can be used to predict the observed ratchet strains shown in Fig. (10c). The full solution map shown in Fig.(8) is constructed on the basis of the montonic properties of 304SS at an average temperature of 900 °F, [8]. It is seen that the operating conditions of the test lie in the ratchetting regime R_3. The cyclic accumulation of ratchet strain is shown as dotted lines in Fig. (10c). It is seen that the predicted strain is quite large compared with observed strain. This over-estimation is attributed to the use of the monotonic data coupled with the kinematic hardening rule which ignores the cyclic hardening behaviour exhibited by the tube material under conditions of reversed strain [17]. An approximate means by which cyclic hardening can be taken into account is to use the monotonic properties during the first cycle only while analysis of subsequent cycles utilizes the 13th cycle yield stress as obtained from an uniaxial push-pull test conducted at an average plastic strain range $\pm \Delta\varepsilon_p$ representive of the operating conditions in the ratchetting test. An estimate of $\Delta\varepsilon_p$ can be evaluated on the basis of the predictions based on monotonic data.

Time dependent creep strains will accumulate during the hold periods at 1100 °F. An upper bound on creep strain per cycle can be determined once the cyclic stress field under rapid thermla shocks is known as shown by Ainsworth [14,15]. This technique is used here to estimate the creep strain per cycle. The refined predictions for plastic and creep ratchet strains are shown as solid line in Fig. (10c). These are closer to observed strain than previous ones but are still in excess of experimental values by ≃ 40%.

It has to be pointed out at this stage that the uniaxial modelling of the physical biaxial problem is likely to produce conservative predictions. A rough estimate of such conservative may be evaluated by comparing the elastic hoop strains in the biaxial problem with that in the uniaxial model. The elastic hoop strain ε_θ at r = b is:

$$\varepsilon^{e}_{\theta} = \frac{1}{E}\left[\sigma_p(1-0.5\nu) - (1-\nu).\ (1-h)\sigma_t\right] \qquad (17a)$$

and the uniaxial strain in the model ε^{e}_{m} at x = 0 is;

$$\varepsilon^{e}_{m} = \frac{1}{E}\left[\sigma_p - (1-h)\sigma_t\right] \qquad (17b)$$

For the operating conditions of Corum's tests, $\varepsilon^{e}_{\theta} = 0.61\ \varepsilon^{e}_{m}$. Applying this ratio to the present predictions of the uniaxial model yields a very close estimate to observed strains.

CONCLUSIONS

The results obtained in the present work provide the transient and steady state solutions for the stress and strain fields in an uniaxial model of a thin tube under combined pressure and cyclic thermal stresses. Analytical expressions are developed for cyclic stresses and ratchet strain using the kinematic hardening plasticity theory.

It is shown that the bilinear temperature distribution across the tube wall intrduces new modes of cyclic plastic deformation in which cyclic plasticity is confined to the inner skin of the tube. Linear distributions of temperature will not exhibit such behaviour. Increasing bilinearity is shown to introduce more stringent ratchetting limits, larger ratchet strains and cyclic plasticity amplitudes at the inner surface of the tube.

The uniaxial model of thin tubes is shown to yield conservative estimates of ratchet strains in the test data of Corum et al [10]. It is demonstrated that proper predictions of ratchet strains should take into account the cyclic hardening phenomenon of metals. An approximate method is used in the present work to assess the effect of cyclic hardening on ratchet strains.

ACKNOWLEDGEMENTS

This work was initiated while the author was at the University of Leicester, England, U.K. Financial support from UKAEA is gratefully acknowledged.

REFERENCES

[1] Kraus, H., Creep Analysis, John Wiley & Sons (1980).

[2] Parkes, E.W., "Structural Effects of Repeated Thermal Loading", Thermal Stress, Benham et al, Pitman and Son's Ltd, London (1964).

[3] Miller, P.R., "Thermal Stress Ratchet Mechanism in Pressure Vessels", J. Basic Engineering, Trans. ASME, 81, 90-196, (1959).

[4] Burgreen, D., "The Thermal Ratchet Mechanism", J. Basic Engineering, Trans. ASME, 90, 469-475(1968).

[5] Bree, J., "Elastic-Plastic Behaviour of Thin Tubes Subjected to Internal Pressure and Intermittent High Heat Fluxes with Applications to Fast-Nuclear-Reactor Fuel Elements", J. Strain Analysis, 2, 226-238(1967).

[6] Megahed, M.M. and Eleiche, A.M, "Cyclic Phenomena in Metals and Their Implications on Structural Behaviour", in Current Advances in Mechanical Design and Production, Proceedings of the 2nd MDP Conference, 403-413,Cairo (1982).

[7] Mulcahy, T.M., "An Assessment of Kinematic Hardening Thermal Ratchetting", J. Engineering for Materials and Technology, Trans. ASME, 96, 214-221(1974).

[8] Megahed, M.M., "The Influence of Hardening Rule on the Elasto-plastic Behaviour of a simple structure Under Cyclic Loading", Int. J. Mech. Sci, 23, 169-182 (1981).

[9] Uga, T., "An Experimental Study on Thermal Stress Ratchetting of Austenitic Stainless Steel By Three Bar Specimens", Nuclear Engng. and Design, 26, 326-335 (1974).

[10] Corum, J.M, Young, H.C. and Grindell, A.G., "Thermal Ratchetting in Pipes Subjected to Intermittent Thermal Downshocks at Elevated Temperatures", 2nd National Congress on Pressure Vessel and Piping, San Francisco, California (1975).

[11] Yamamoto, S., Kano, J. and Yoshitoshi, A., "Thermal Ratchetting Experiments of Type 304 Stainless Steel Pipes Under Alternating Cold and Hot Thermal Shocks with Varying Axial Load", Elevated Temperature Design Symposium, ASME, New York, 25-32 (1976).

[12] Megahed, M.M., Ponter, A.R.S. and Morrison, C.J., "Experimental Investigations into the Influence of Cyclic Phenomena of Metals on Structural Ratchetting Behaviour" submitted for publication, Int. J. Mech. Sci. (1983).

[13] Megahed, M.M., Ponter, A.R.S. and Morrison, C.J, "Ratchetting Tests on 316 Stainless Steel Strutures at Room and 400 °C", to be published.

[14] Ainsowrth, R.A., "Bounding Solutions for Creeping Structures subjected to Load Variations Above the Shakedown Limit", Int. J. Solids and Structures, 13, 971-980(1977).

[15] Ainsworth, R.A., "Applications of Bounds for Creeping Structures Subjected to Load Variations above the Shakedown Limit", Int. J. Solids and Structures, 13, 981-993 (1977).

[16] Timoshenko, S. and Goodier, J.N., "Theory of Elasticity," McGraw Hill (1970).

[17] "Mechanical Properties Test Data for Structural Materials," Atomic Energy Commission, U.S. ORNL, 4948(1974).

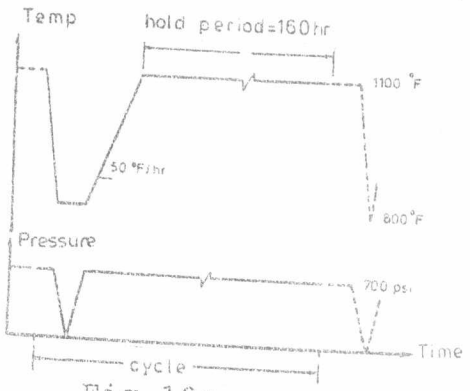

Fig.10a

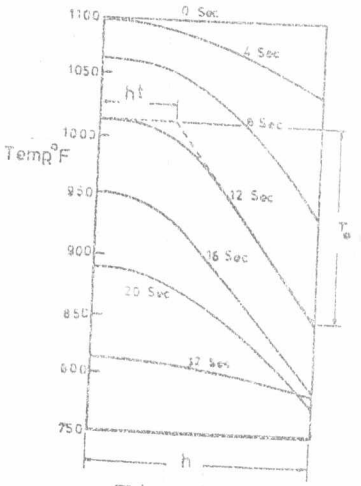

Fig.10b

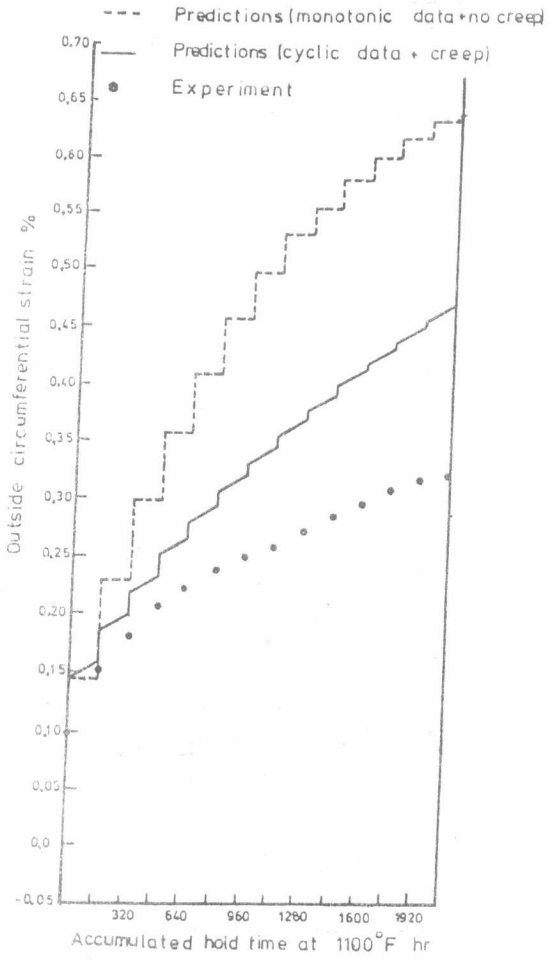

Fig.10c

Fig.10a. Load histogram

Fig.10b. Transient temperature distribution across the tube wall [10].

Fig.10c. Comparison between model prediction and experimental results.